Journal of Heat and Mass Transfer Research 5 (2018) 39– 49

Journal of Heat and Mass Transfer Research

Journal homepage: http://jhmtr.journals.semnan.ac.ir

Semnan University

Numerical study of a combined convection flow in a cavity filled with nanofluid considering effects of diameter of nanoparticles and cavity inclination angles

Mohammad Hemmat Esfe*, Seyfolah Saedodin

Faculty of mechanical engineering, Semnan University, Semnan, Iran

PAPER INFO

History:

Submitted:2016-06-20
Revised:2017-01-13
Accepted:2017-02-04

Keywords :

Nanofluid;
Variable properties;
Solid volume fraction;
lid- driven cavity;
Diameter of nanoparticles.

A B S T R A C T

The present paper focuses on problem of mixed convection fluid flow and heat transfer of Al2O3-water nanofluid with temperature and nanoparticles concentration dependent thermal conductivity and effective viscosity inside Lid-driven cavity having a hot rectangular obstacle. The governing equations are discretized using the finite volume method while the SIMPLER algorithm is employed to couple velocity and pressure fields. Using the developed code, the effects of cavity inclination angle, diameter and solid volume fraction of the Al2O3 nanoparticles on the flow and thermal fields and heat transfer inside the cavity are studied. The results show that at all solid volume fraction the average Nusselt number has inverse relationship with nanoparticles diameter. Also the results have clearly indicated that with increasing slope of the cavity to 90 degree, heat transfer continuously decreases at all studied Richardson numbers© 2017 Published by Semnan University Press. All rights reserved.

© 2018 Published by Semnan University Press. All rights reserved.

DOI: 10.22075/jhmtr.2017.1503.1100

1. Introduction

Suspending nanoparticles in a host fluid will result in a new fluid that is called nanofluid. Water, Ethylene glycol and propylene glycol are from famous host fluids. In 1995 Choi et al. introduced new age of fluids that now is known as nanofluid. Existence of high thermal conductivity metallic nanoparticles (e.g., copper, aluminum, silver and Titanium) increases the thermal conductivity of such mixtures, thus enhancing their overall heat transfer capability (Xuan et al. 2003). In recent years, Nanofluids have attracted attention as a new innovation of heat transfer fluids in building heating, in various heat exchangers, in plants and in automotive cooling applications, because of their excellent thermal performance. Various benefits of the application of nanofluids include: improved heat transfer, heat transfer system size reduction, minimal clogging, micro channel cooling and miniaturization of systems (Choi, 1995).

Numerous investigates have been conducted on the thermophysical properties of nanofluids (effective dynamic viscosity, thermal conductivity and etc.) and the energy transport in nanofluids. Study of thermophysical properties of nanofluids can be observed in several literatures such as Lee et al. (2000), Xie et al. (2002), Patel et al. (2005), and Chang et al. (2005), Also many theoretical, numerical simulations and empirical studies on influence of existence of nanoparticle in convective heat transfer have been reported.

On the other hand, fluid flow and heat transfer in a cavity filled by pure fluid which is driven by buoyancy and shear have been studied extensively in literature. Mixed Convection (a kind of convection Including natural convection heat

Corresponding Author : *M. Hemmat Esfe, Faculty of mechanical engineering, Semnan University, Semnan, Iran*
Email : M.hemmatesfe@gmail.com

transfer and forced convection heat transfer) has significant role in many applications in industry and engineering. lake and reservoirs (Imberger and Hamblin, 1982), food processing, crystal growth (Moallemi and Jang, 1992), electronic cooling devices, drying technologies, solar ponds (Cha and Jaluria, 1984) solar collectors(Ideriah, 1980) and float glass production (Pilkington, 1969), are among its current applications .

Effect of several parameters on mixed convection of various cavities are investigated in many studies like Talebi et al. (2010), Abunada et al.(2010), Mahmoodi(2011), Sadodin et al.(2011), Hemmat Esfe et al.(2012), Abbasian Arani et al.(2012), Hemmat Esfe (2012), Fereidoon et al.(2013), Saedodin et al.(2013) and Zarei et al.(2013). They studied effects of parameters like cavity geometry, base fluid and effect of boundary condition etc.

Nikfar and Mahmoodi (2012) simulated natural convection in a square cavity containing water based nanofluid. They stated that Nusselt number of cavities hot wall has direct relationship with solid volume fraction.

In another study Mahmoodi and Mazrouei(2012) studied the effect of putting adiabatic obstacles in cavities on fluid flow and natural heat transfer. The working fluid in their study was a water based fluid containing Cu nanoparticles. They stated that at low Rayleigh numbers, the rate of heat transfer reduces by increasing the size of adiabatic obstacles.

Mahmoodi (2012) studied mixed convection in a lid-driven cavity filled with Al_2O_3-water nanofluid. Having a moving top wall in their simulation is one of their novelties in their study. In another research Mazrouei and Sebdani et al.(2012) checked the variable properties of nanofluids effect on mixed convection in a rectangular cavity.

In present study an inclined square cavity is simulated in order to study the mixed convection of flow in a cavity filled with Al_2O_3 nanoparticles and also with a heated obstacle and upper moving walls. Based on the authors' knowledge no research or paper has been done or publish in cavity with Simultaneous changes in parameters such as diameter of nanoparticles and inclination angles. The effects of changes in important parameters such as Richardson number, inclination angle, diameter of nanoparticles and solid volume concentration of the Al2O3 nanoparticles on the flow and thermal fields and heat transfer inside the cavity with heated obstacle has not been reported so far. Utilizing of new variable properties models for estimate the thermal conductivity and dynamic viscosity of nanofluid are other aspects that distinguished this survey from other numerical studies in this domain.

2. Physical modeling

In Fig. 1 a schematic of studied geometry in present study can be seen. As it stated the cavity contains a water based nanofluid with Al_2O_3 nanopartilces. Adiabatic condition is considered for left, top and bottom sides of cavity. For the right wall of cavity a low temperature like Tc is considered. Also Th is determined as temperature of obstacle in order to induce the buoyancy effect.

The nanofluid behavior used in cavity is Newtonian, Incompressible and the flow is laminar. Also it is considered that the host fluid and nanoparticles as solid phase, flow with the same velocity in cavity. The density variation in the body force term of the momentum equation is satisfied by Boussinesq's approximation. The thermophysical properties of nanoparticles and the water as the base fluid at T = 25˚C are presented in Table1.

The thermal conductivity and the viscosity of the nanofluid are taken into consideration as variable properties; both of them change with volume fraction and temperature of nanoparticles. Under the above assumptions, the system of governing equations is:

$$\frac{\partial u}{\partial x}+\frac{\partial v}{\partial y}=0, \tag{1}$$

Table 1. Thermophysical properties of all ingredients of nanofluid at T =25˚C.

Physical properties	Fluid phase (Water)	Solid (Al_2O_3)
C_p(J/kg k)	4179	765
ρ (kg/m3)	997.1	3970
K (W m-1 K-1)	0.6	25
$\beta\times10^{-5}$ (1/K)	21.	0.85
$\mu\times10^{-4}$(Kg/ms)	8.9	……..
d_p (nanometer)	---	47

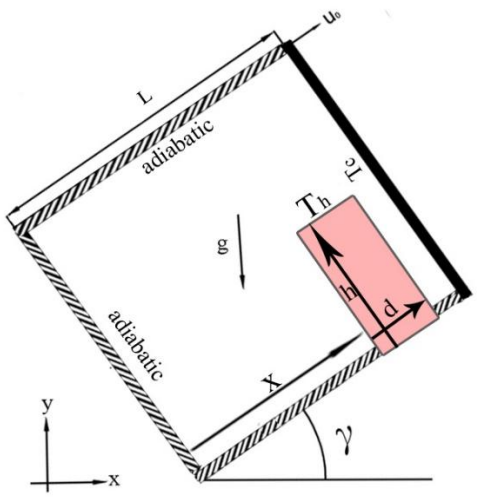

Fig. 1. Schematic diagram of current study

$$u\frac{\partial u}{\partial x}+v\frac{\partial u}{\partial y}=-\frac{1}{\rho_{nf}}\frac{\partial p}{\partial x}+\upsilon_{nf}\nabla^2 u+\frac{(\rho\beta)_{nf}}{\rho_{nf}}g\Delta T.Sin(\gamma) \tag{2}$$

$$u\frac{\partial v}{\partial x}+v\frac{\partial v}{\partial y}=-\frac{1}{\rho_{nf}}\frac{\partial p}{\partial y}+\upsilon_{nf}\nabla^2 v+\frac{(\rho\beta)_{nf}}{\rho_{nf}}g\Delta T.Cos(\gamma) \tag{3}$$

and

$$u\frac{\partial T}{\partial x}+v\frac{\partial T}{\partial y}=\alpha_{nf}\nabla^2 T. \tag{4}$$

The dimensionless parameters may be presented as

$$X=\frac{x}{L},\ Y=\frac{y}{L},\ V=\frac{v}{u_0},\ U=\frac{u}{u_0}$$

$$\Delta T=T_h-T_c,\ \theta=\frac{T-T_c}{\Delta T},\ P=\frac{p}{\rho_{nf}u_0^2}. \tag{5}$$

Hence,

$$\mathrm{Re}=\frac{\rho_f u_0 L}{\mu_f},\ Ri=\frac{Ra}{\mathrm{Pr}.\mathrm{Re}^2},\ Ra=\frac{g\beta_f\Delta TL^3}{\upsilon_f\alpha_f},\ \mathrm{Pr}=\frac{\upsilon_f}{\alpha_f}. \tag{6}$$

The dimensionless form of the above governing equations (1) to (4) become

$$\frac{\partial U}{\partial X}+\frac{\partial V}{\partial Y}=0 \tag{7}$$

$$U\frac{\partial U}{\partial X}+V\frac{\partial U}{\partial Y}=-\frac{\partial P}{\partial X}+\frac{\upsilon_{nf}}{\upsilon_f}\frac{1}{\mathrm{Re}}.\nabla^2 U+\frac{Ri}{\mathrm{Pr}}.\frac{\beta_{nf}}{\beta_f}\Delta\theta.\sin(\gamma) \tag{8}$$

$$U\frac{\partial V}{\partial X}+V\frac{\partial V}{\partial Y}=-\frac{\partial P}{\partial Y}+\frac{\upsilon_{nf}}{\upsilon_f}\frac{1}{\mathrm{Re}}.\nabla^2 V+\frac{Ri}{\mathrm{Pr}}.\frac{\beta_{nf}}{\beta_f}\Delta\theta.\cos(\gamma) \tag{9}$$

and

$$U\frac{\partial\theta}{\partial X}+V\frac{\partial\theta}{\partial Y}=\frac{\alpha_{nf}}{\alpha_f}\nabla^2\theta \tag{10}$$

2.1 Thermal diffusivity and effective density

Thermal diffusivity and effective density of the nanofluid are

$$\alpha_{nf}=\frac{k_{nf}}{(\rho c_p)_{nf}} \tag{11}$$

$$\rho_{nf}=\varphi\rho_s+(1-\varphi)\rho_f \tag{12}$$

2.2 Heat capacity and thermal expansion coefficient

Heat capacity and thermal expansion coefficient of the nanofluid are therefore

$$(\rho c_p)_{nf}=\varphi(\rho c_p)_s+(1-\varphi)(\rho c_p)_f \tag{13}$$

$$(\rho\beta)_{nf}=\varphi(\rho\beta)_s+(1-\varphi)(\rho\beta)_f \tag{14}$$

2.3 Viscosity

The effective viscosity of nanofluid was calculated by:

$$\mu_{\mathrm{eff}}=\mu_{\mathrm{f}}(1+2.5\varphi)\left[1+\eta\left(\frac{d_p}{L}\right)^{-2\varepsilon}\varphi^{2/3}(\varepsilon+1)\right] \tag{15}$$

This well-validated model is presented by Jang et al. (2007) for a fluid containing a dilute suspension of small rigid spherical particles and it accounts for the slip mechanism in nanofluids. The empirical constant ε and η are -0.25 and 280 for Al2O3, respectively.

It is worth mentioning that the viscosity of the base fluid (water) is considered to vary with temperature and the flowing equation is used to evaluate the viscosity of water,

$$\mu_{H_2O}=(1.2723\times T_{rc}^{\ 5}-8.736\times T_{rc}^{\ 4}+33.708\times T_{rc}^{\ 3}-246.6\times T_{rc}^{\ 2}+518.78\times T_{rc}+1153.9)\times 10^{6}$$

where $T_{rc}=Log(T-273)$ (16)

2.4 Dimensionless stagnant thermal conductivity:

Hamilton and crosser (H-C model)(1962), is used for calculating effective thermal conductivity of suspended nanoparticles in a host fluid.

$$\frac{k_{stationary}}{k_f}=\frac{k_s+2k_f-2\varphi(k_f-k_s)}{k_s+2k_f+\varphi(k_f-k_s)} \tag{17}$$

2.5 Total dimensionless thermal conductivity of nanofluids:

$$\frac{k_{nf}}{k_f}=\frac{k_{stationary}}{k_f}+\frac{k_c}{k_f}=\frac{k_s+2k_f-2\varphi(k_f-k_s)}{k_s+2k_f+\varphi(k_f-k_s)}+c\frac{Nu_p d_f(2-D_f)D_f}{\mathrm{Pr}(1-D_f)^2}\frac{\left[\left(\frac{d_{\max}}{d_{\min}}\right)^{1-Df}-1\right]^2}{\left(\frac{d\max}{d\min}\right)^{2-Df}-1}\frac{1}{d_p} \tag{18}$$

The presented model is achieved by results of Xu et al. (2006) study and has been chosen to reach the thermal conductivity of nanofluids. In presented formula "c" is an experimental constant that is a certain number for each host fluid. It is 85 for deionized water and is 280 for ethylene glycol. This constant is not related to type of nanoparticles.
Nup is the Nusselt number for liquid flowing around a spherical particle and equal to two for a single particle. The fluid molecular diameter is df =4.5*10-10(m) for water in present study and the fractal dimension Df is determined by:

$$D_f = 2 - \frac{\ln \varphi}{\ln\left(\frac{d_{p,\min}}{d_{p,\max}}\right)} \tag{19}$$

where dp,max and dp,min are the maximum and minimum diameters of nanoparticles, respectively. Ratio of minimum to maximum nanoparticles dp,min/dp,max is R.

$$d_{p,\max} = d_p . \frac{D_f - 1}{D_f}\left(\frac{d_{p,\min}}{d_{p,\max}}\right)^{-1}$$
$$d_{p,\min} = d_p . \frac{D_f - 1}{D_f} \tag{20}$$

3. Numerical approach

Governing equations for continuity, momentum and energy equations associated with the boundary conditions in this investigation were calculated numerically based on the finite volume method and associated staggered grid system, using FORTRAN computer code. The SIMPLER algorithm is used to solve the coupled system of governing equations. The convection terms is approximated by a hybrid-scheme which is conducive to a stable solution. In addition, a second-order central differencing scheme is utilized for the diffusion terms. The algebraic system resulting from numerical discretization was calculated utilizing TDMA applied in a line going through all volumes in the computational domain. The solution process is repeated until an acceptable convergence criterion is reached. A FORTRAN computer code has been developed to solve the equations as described above. The process is repeated until the following convergence criterion is satisfied:

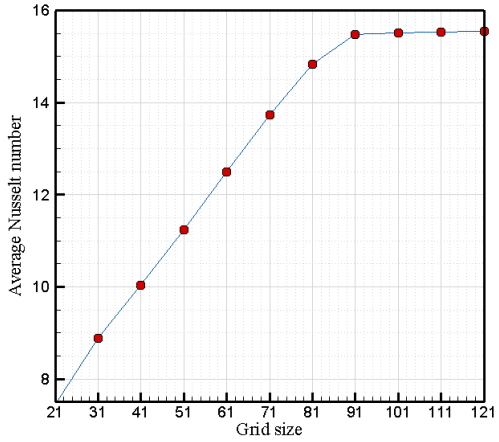

Fig. 2. Mesh valid at X=0.6L, φ=0.05, γ=90˚

$$error = \frac{\sum_{j=1}^{j=M}\sum_{i=1}^{i=N}\left|\lambda^{n+1} - \lambda^{n}\right|}{\sum_{j=1}^{j=M}\sum_{i=1}^{i=N}\left|\lambda^{n+1}\right|} < 10^{-7} \tag{21}$$

In above equation, M and N are number of grid points in x and y directions, respectively. n shows number of iteration and λ is representative of any scalar transport quantity. Nine different mesh sizes were used to check and qualify the grid independency.
As can be observed, 101 × 101 uniform grid size yields the required accuracy and was hence applied for all simulation exercises in this work as presented in the following section.
To ensure the accuracy and validity of this new model, we analyze a square cavity filled with base fluid with Pr = 0.7 and different Ra numbers. Table 2 shows the comparison between the results obtained with our research and the values presented in the literature. The quantitative comparisons for the average Nusselt numbers indicate an excellent agreement between them.

Table 2. Validation analysis results

	Present study	Hadjisophocleous	Tiwari and Das	Fusegi et al.	Ha et al.
Ra=103					
Nu	1.1366	1.141	1.0871	1.085	1.072
Numax	1.5738	1.540	1.508		
Numin	0.6468	0.727	0.6901		
Ra=104					
Nu	2.3256	2.29	2.195	2.1	2.070
Numax	3.5456	3.84	3.5585		
Numin	0.7172	0.670	0.5809		
Ra=105					
Nu	4.4928	4.964	4.450	4.361	4.464
Numax	7.3037	8.93	7.9371		
Numin	0.9906	1.01	0.7173		
Ra=106					
Nu	8.6388	10.39	8.803		
Numax	14.2521	21.41	19.2675		
Numin	1.6247	1.58	0.9420		

4 .Results and discussion

In this study, thermal characteristics and flow patterns inside an inclined cavity filled with nanofluid with hot barrier are investigated. Some parameters such as diameter of nanoparticles, cavity inclination angles, solid volume fraction and Richardson number are considered and their effects on streamlines, isotherms and total heat transfer are studied. Grashof number is assumed constant and equal to 104 while

Figure 3 shows flow and temperature behavior in different cavity inclination angles at. Flow pattern for horizontal situation of the cavity shows presence of a clockwise primary cell in upper parts of the cavity while one small vortex is formed at right side of hot barrier. Presence of vortexes results from two buoyancy force due to temperature difference and shear force due to upper lid movement. In horizontal situation, buoyancy and shear forces assist each other. With increasing slope of this cavity, buoyancy acts in a direction opposite to shear forces and formation of a small vortex near upper lid proves this fact. It is expected that increasing cavity inclination angles to 90oresults in relative neutralization of buoyancy forces and shear forces and consequently vortex forces and heat transfer inside the cavity decrease. Isotherm lines in horizontal position of the cavity also show density of lines near isotherm walls. With increasing slope of the cavity, density of isotherm lines and thereupon temperature gradient near walls decrease and this decrease is expected to reduce heat transfer inside the cavity.

Figure 4 portrays streamlines and isotherms to demonstrate the effect of nanoparticles diameter for Ri=1, T=300 and . 4 different diameters (20, 40, 60 and 80 nano meter) are shown in this figure. As it is observed, changes in nanoparticles diameter produces no substantial changes in flow patterns and temperature. Flow pattern in this parameter range shows formation of two clockwise and anti-clockwise vortexes which upper clockwise vortex is stronger than lower and occupies more spaces of the cavity. The strength of vortexes slightly decreases with increasing nanoparticles diameter but their core and primary form is maintained. Temperature lines also demonstrate formation of a thermal boundary layer inside the cavity and near the barrier. Isotherm lines are slightly separated from each other with increasing diameter of nanoparticles and therefore, temperature gradient decreases. According to isotherm lines it is expected that increasing diameter of nanoparticles causes total heat transfer inside the cavity to decrease slightly.

Variation of isotherms and streamlines versus volume fraction of nanoparticle inside the cavity are demonstrated in figure 5 at Ri=0.01, dp=40, T=300, . Streamlines show formation of a strong vortex in upper and middle parts of the cavity while two strong and weak vortexes can be observed at sides of hot rectangular barrier. No significant changes occur in flow pattern with increasing volume fraction of nanoparticles. Temperature lines in this range of parameters present intense density of isotherm lines near isothermal walls. Density of lines decreases very slightly with increasing volume fraction and temperature gradient reduces. Despite a reduction in temperature gradient with increasing volume fraction, no accurate prediction can be made for total heat transfer inside the cavity. Increasing solid concentration increases thermal conductivity of nanofluid while it slightly decreases temperature gradient.

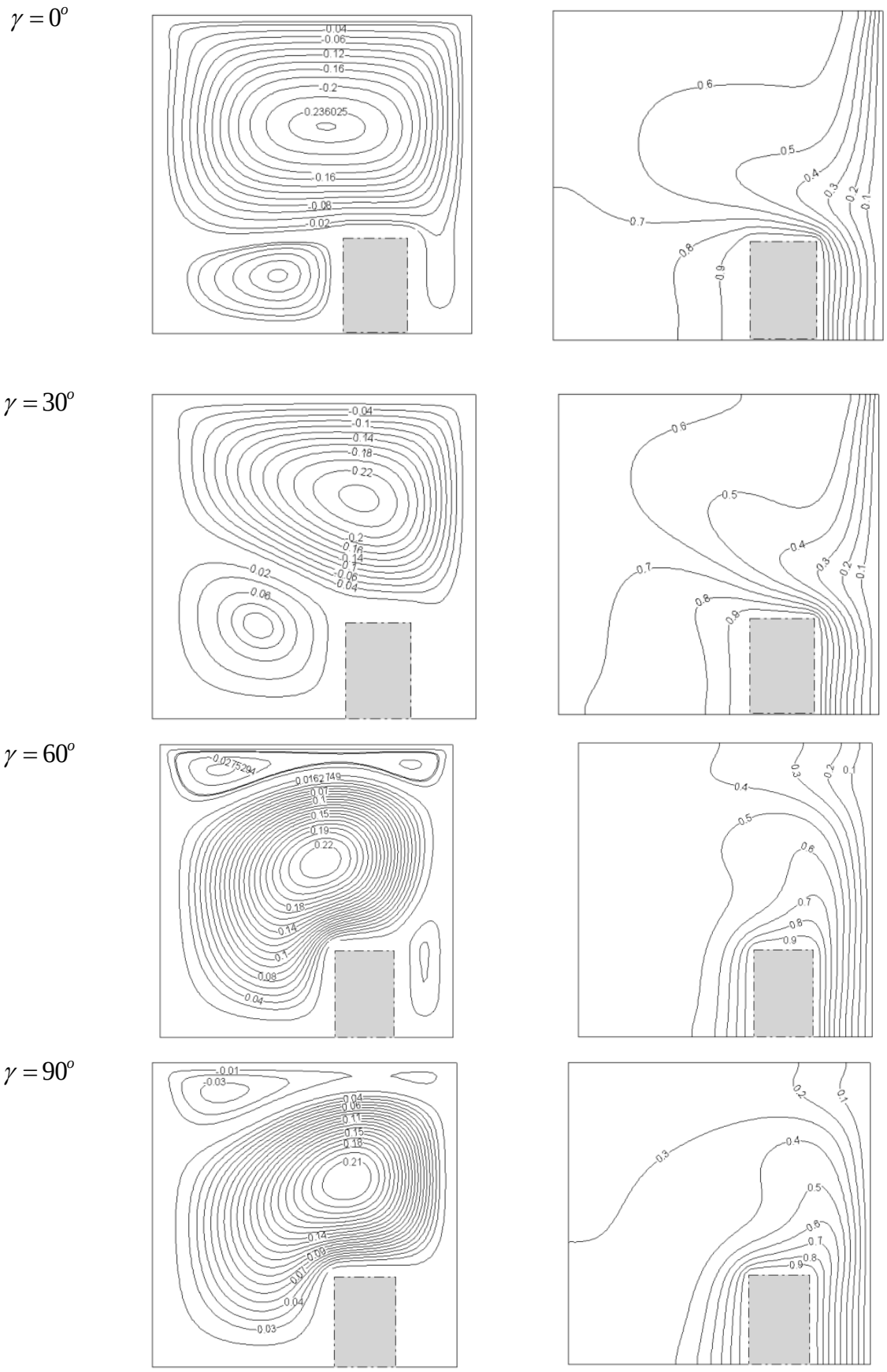

Fig. 3. streamlines and isotherms in different inclination angles in Ri=100, φ=0.05%, d_p=20 nm

d_p=20 nanometer

d_p=40 nanometer

d_p=60 nanometer

d_p=80 nanometer

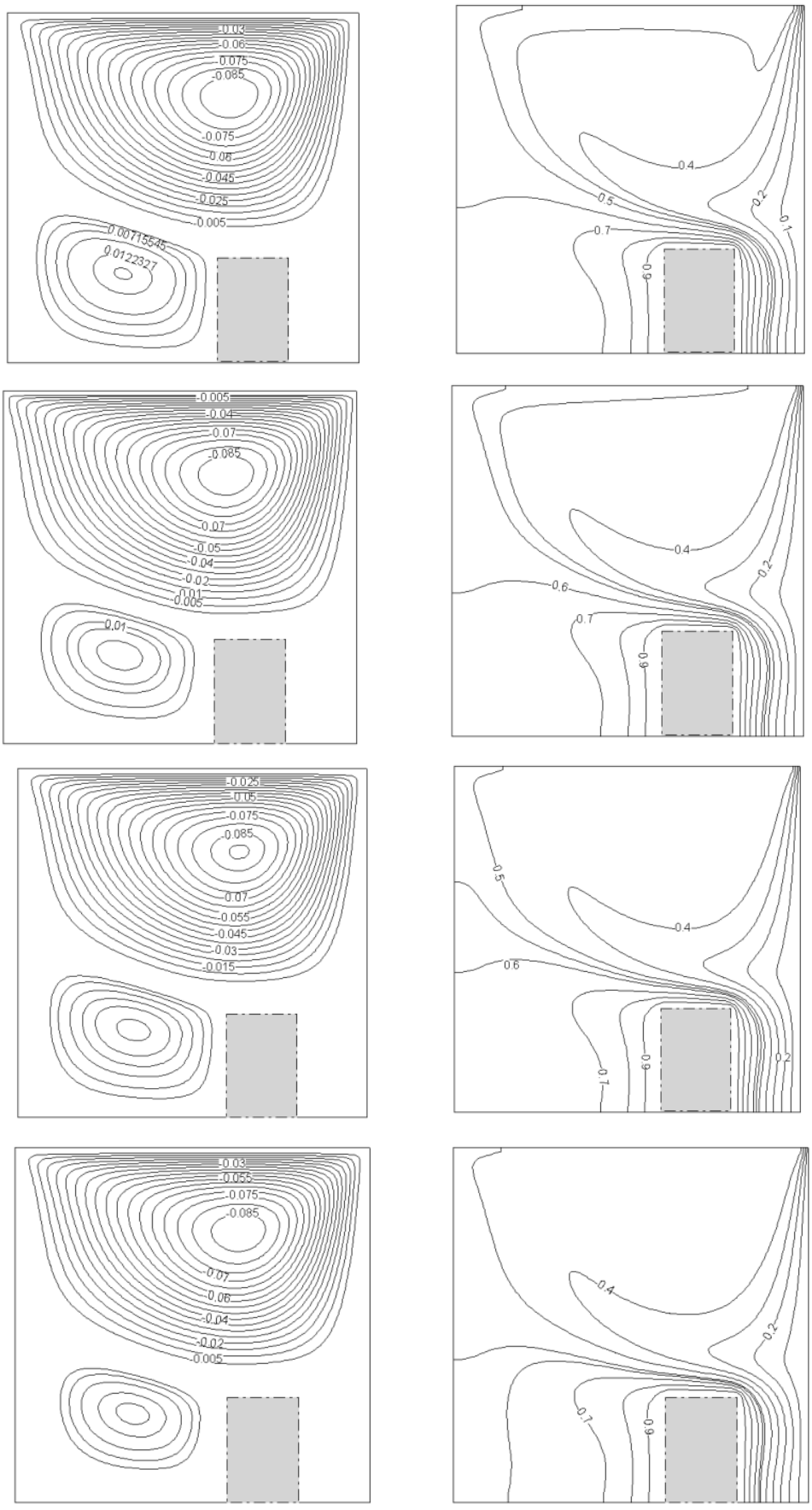

Fig. 4. streamlines and isotherms in different diameter of nanoparticles at Ri=1, φ=0.05%, T=300, γ=30

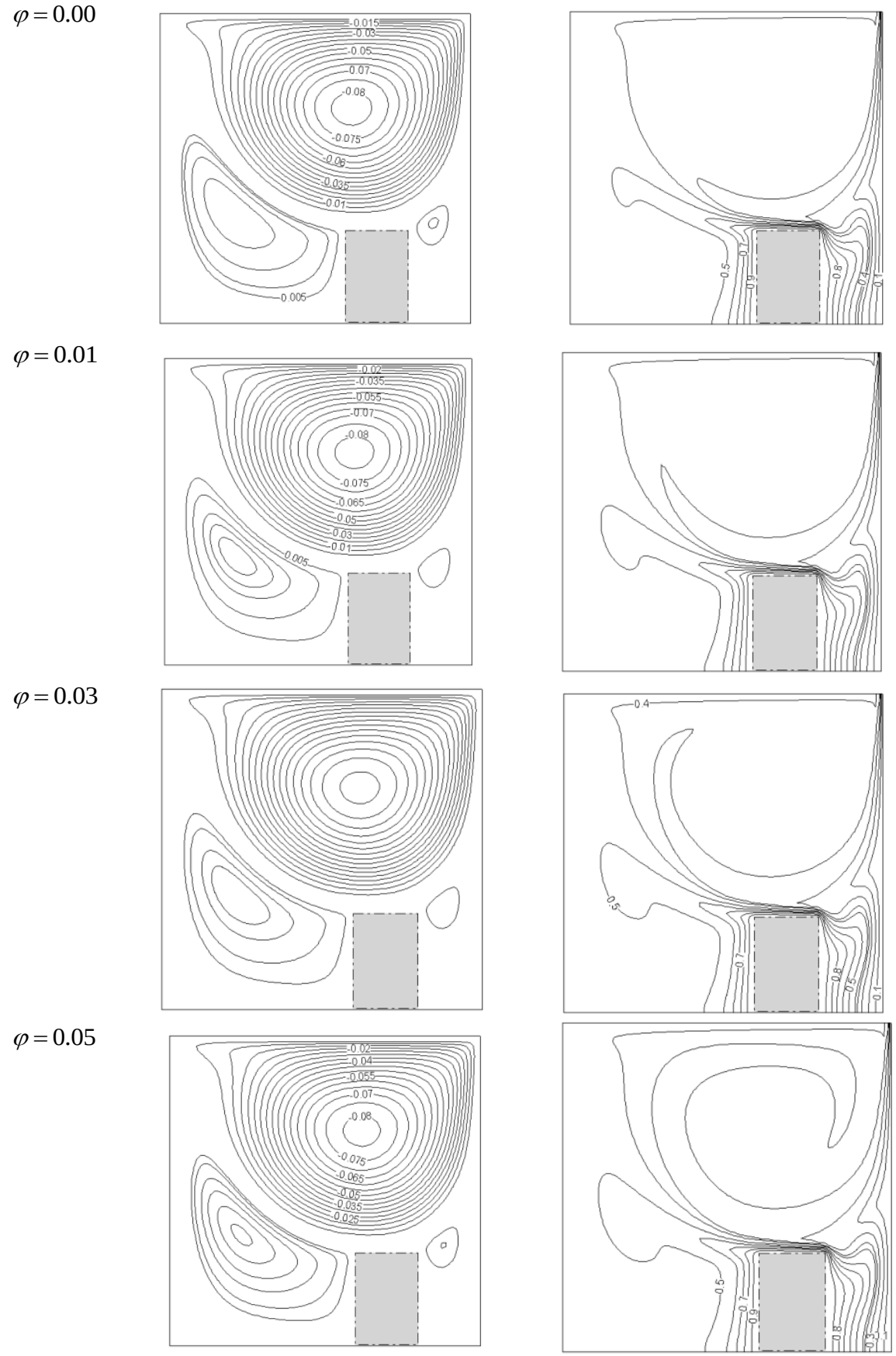

Fig. 5. streamlines and isotherms in different solid volume concentration at Ri=0.01, dp=40, T=300, $\gamma = 60^o$

Figure 6 illustrates heat transfer inside the cavity versus changes of slope and Richardson number for dp=20, T=300, . As it is obvious in this diagram, with increasing Richardson number and (buoyancy forces dominate shear force) Nusselt number and consequently heat transfer inside the cavity decrease. On the other hand, with increasing cavity inclination angles from horizontal position, buoyancy force and shear force counteract each other and as a result total heat transfer inside the cavity decreases. This matter was discussed earlier when figure 2 was studied.

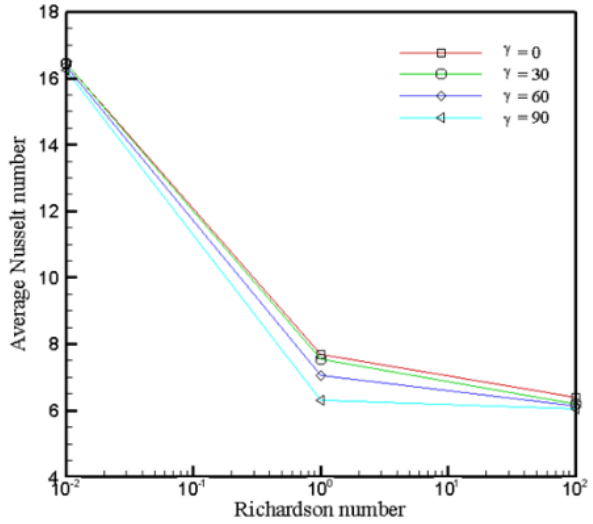

Fig. 6. Variation of Nusselt number versus cavity inclination angle and Richardson number for dp=20, T=300, $\varphi = 0.05$.

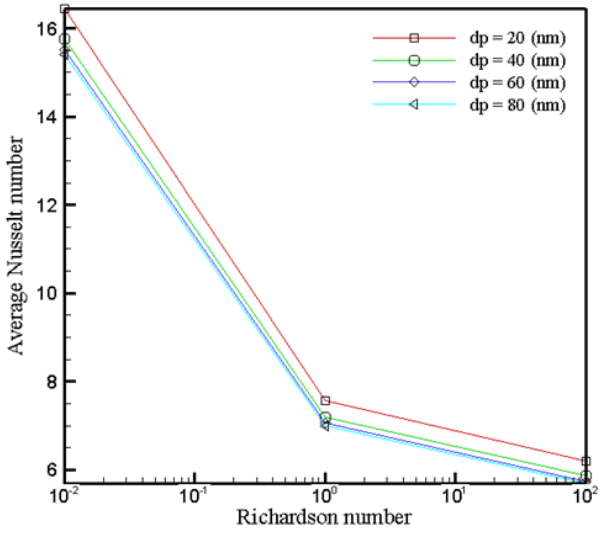

Fig. 7. Variation of Nusselt number versus Richardson number for different diameters of nanoparticles dispersed in water for T=300º, $\gamma = 30^o$ and $\varphi = 0.05$ %

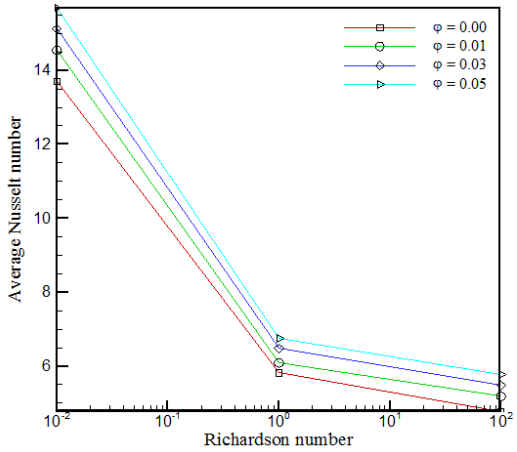

Fig. 8. Variation of Nusselt number versus Richardson number and volume fraction of nanoparticles at d_p=40, T=300º and $\gamma = 60^o$

Figure 7 shows variation of Nusselt number versus Richardson number for different diameters of nanoparticles dispersed in water for T=300o, and . At this condition, values of Nusselt number for all diameters of nanoparticles decrease with increasing Richardson number. With increasing nanoparticles diameter from 20 nm to 40 nm, a relatively significant change occurs in heat transfer while with increasing diameter more than 40 nm, no significant changes occur in heat transfer and Nusselt number. Figure 8 illustrates variation of Nusselt number versus changes in Richardson number and volume fraction of nanoparticles at dp=40, T=300o and . As it is seen in this diagram, adding nanoparticles to base fluid causes a considerable increase in heat transfer inside the cavity and this increasing trend continues with increasing volume fraction. On the other side, in this range of parameters increasing Richardson number (i.e. buoyancy force dominates shear force) also results in a reduction in Nusselt number and consequently heat transfer inside the cavity.

5. Conclusion

In this paper thermal behavior of nanoparticles inside an inclined cavity with a hot barrier was investigated. Effects of some important parameters including nanoparticle diameter, cavity inclination angles, volume fraction and Richardson number were studied and below results were obtained:

1- With increasing Richardson number and predominance of buoyancy force over shear force, Nusselt number and heat transfer decrease.

2- In horizontal situation that buoyancy and shear forces have the same direction, the maximum values are obtained for Nusselt number and heat transfer.

3- With increasing slope of the cavity to 90 degree, heat transfer continuously decreases at all studied Richardson numbers.

4- With decreasing diameter of dispersed nanoparticles in water, heat transfer increases.
5- Adding nanoparticles to base fluid in addition to maintaining flow pattern causes a significant increase in heat transfer inside the cavity.

Nomenclature

specific heat, J kg^{-1} K^{-1}
Grashof number
gravitational acceleration, m s^{-2}
heat transfer coefficient, W m^{-2} K^{-1}
enclosure length, m
thermal conductivity, W m^{-1} K^{-1}
Nusselt number
pressure, N m^{-2}
dimensionless pressure
Prandtl number
heat flux, W m^{-2}
Reynolds number
Richardson number
dimensional temperature, K
dimensional velocities components in x *and* y *direction, m s^{-1}*
dimensionless velocities components in X and Y direction
lid velocity
dimensional Cartesian coordinates, m
dimensionless Cartesian coordinates

Greek symbols

α	*thermal diffusivity, m^2 s*
β	*thermal expansion coefficient, K^{-1}*
θ	*dimensionless temperature*
μ	*dynamic viscosity, Kg m^{-1} s^{-1}*
ν	*kinematic viscosity, m^2 s^{-1}*
ρ	*density, kg m^{-3}*
φ	*volume fraction of the nanoparticles*

Subscripts

c	*cold*
eff	*effective*
f	*fluid*
h	*hot*
nf	*nanofluid*
s	*solid particles*
w	*wall*

References

[1]. Choi, S.U.S.(1995) Enhancing thermal conductivity of fluids with nanoparticles, developments and applications of non-Newtonian flows, in: D.A. Siginer, H.P. Wang (Eds.), FEDvol. 231/MDvol. 66, The American Society of Mechanical Engineers, New York, 99-105.

[2]. Xuan, Y., Li, Q., (2003). Investigation on convective heat transfer and flow features of nanofluids. Journal of Heat Transfer, 125, 151–155.

[3]. Lee, S., Choi, S.U.S., Li, S., & Eastman, J.A. Measuring Thermal Conductivity of Fluids Containing Oxide Nanoparticles". International Journal of Heat and Mass Transfer,.121, 280-289.

[4]. Xie, H.Q., Wang, J.C., Xi, T.G., Li, Y., & Ai, F., (2002). Dependence of the thermal conductivity of nanoparticle–fluid mixture on the base fluid. J. Mat. Sci. Let., 21, 1469–1471.

[5]. Patel, H.E., Pradeep, T., Sundararajan, T., Dasgupta, A., Dasgupta, N.,& Das, S.K., (2005). A micro convection model for thermal conductivity of nanofluid. Pramana-Journal of Physics, 65, 863–869.

[6]. Chang, H., Jwo, C.S., Lo, C.H., Tsung, T.T., Kao, M.J.,& Lin H.M., (2005). Rheology of CuO nanoparticle suspension prepared by ASNSS. Reviews on Advanced Materials Science, 10, 128–132.

[7]. Imberger, J., & Hamblin, P.F. (1982). Dynamics of lakes, reservoirs, and cooling ponds. Annual Rev. Fluid Mech. 14, 153–187.

[8]. Moallemi, M.K., & Jang, K.S. (1992). Prandtl number effects on laminar mixed convection heat transfer in a lid-driven cavity. Int. J. Heat Mass Transfer. 35, 1881– 1892.

[9]. Cha, C.K., & Jaluria, Y. (1984). Recirculating mixed convection flow for energy extraction. Int. J. Heat Mass Transfer. 27, 1801–1810.

[10]. Ideriah, F.J.K. (1980). Prediction of turbulent cavity flow driven by buoyancy and shear. J. Mech. Eng. Sci. 22, 287–295.

[11]. Pilkington, L.A.B. (1969). Review lecture: the float glass process. Proc. Roy. Soc. Lond A . 314, 1–25.

[12]. Talebi, F., Mahmoudi, A.H. & Shahi, M. (2010). Numerical study of mixed convection flows in a square lid–driven cavity utilizing nanofluid. Int. Commun. Heat Mass.37 79–90.

[13]. Abu–Nada, E., & Chamkha, A.J., (2010). Mixed convection flow in a lid driven square enclosure filled with a nanofluid. Eur. J. Mech. B-Fluid, 29, 472–482.

[14]. Mahmoodi, M., (2011). Mixed convection inside nanofluid filled rectangular enclosures with moving bottom wall. Thermal Science, 15, 889-903.

[15]. Saedodin, S., Hemmat Esfe, M., Noroozi, M.J. (2011). Numerical simulation of mixed convection of fluid flow and hea t transfer within car radiator with an inside obstacle filled with nanofluid, E-Modeling.; Vol. 9 (25), pp. 33-46.

[16]. Hemmat Esfe, M., Ghadak, F., Haghiri, A., Mirtalebi Esforjani, S.,(2012) Numerical Study of Mixed Convection Flows in a Two-sided Inclined Lid-driven Cavity Utilizing Nano-fluid with Various Inclination Angles and Ununiformed Temperature. Aerospace Mechanics Journal.; 8 (2) :69-83.

[17]. Abbasian Arani, A. A., Amani, J., Hemmat Esfe, M., (2012) Numerical simulation of mixed convection flows in a square double lid-driven cavity partially heated using nanofluid, Journal of nanostructure, 2 ,pp. 301-311.

[18]. Hemmat Esfe, M., Saedodin, S., (2012). Flow behavior and thermal performance of double lid-driven cavity subjected to nanofluid with variable properties , E-Modeling, 10(30): 43-60.

[19]. Fereidoon, A., Saedodin, S., Hemmat Esfe, M. and Noroozi, M.J., (2013)Evaluation of mixed convection in inclined square lid driven cavity filled with Al2O3/water nanofluid, Engineering Applications of Computational Fluid Mechanics, 7(1), pp. 55–65.

[20]. Zarei, H., Rostamian, S. H. and Hemmat Esfe, M., (2013) Heat transfer behavior of mixed convection flow in lid driven cavity containing hot obstacle subjected to Nanofluid with variable properties, J. Basic. Appl. Sci. Res., 3(2), pp.713-721.

[21]. Saedodin, S., Biglari, M., Hemmat Esfe, M., Noroozi, M.J., (2013). Mixed Convection Heat Transfer Performance in a Ventilated Inclined Cavity Containing Heated Blocks: Effect of Dispersing Al2O3 in Water and Aspect Ratio of the Block. Journal of Computational and Theoretical Nanoscience Vol. 10, 2663–2675.

[22]. Nikfar, M., & Mahmoodi, M.(2012). Meshless local Petrov–Galerkin analysis of free convection of nanofluid in a cavity with wavy side walls. Eng. Anal. Bound. Elem. 36 ,433–445.

[23]. Mahmoodi, M.,& Mazrouei Sebdani, S., (2012). Natural Convection in a Square Cavity Containing a Nanofluid and an Adiabatic Square Block at the Center. Superlattice Microst. 52, 261-275.

[24]. Mahmoodi, M. (2012). Mixed convection inside nanofluid filled rectangular enclosures with moving bottom wall, Thermal Science.

[25]. Mazrouei Sebdani, S., Mahmoodi, M., & Hashemi, S.M. (2012). Effect of nanofluid variable properties on mixed convection in a square cavity. Int. J. Thermal Sci. 52, 112–126

[26]. Jang, S.P., Lee, J.H., Hwang, K.S., & Choi, S.U.S.(2007). Particle concentration and tube size dependence of viscosities of Al2O3-water nanofluids flowing through micro- and minitubes. Appl. Phys. Lett. 91, 24-31.

[27]. Hamilton, R.L.,& Crosser, O.K.(1962). Thermal conductivity of heterogeneous two component systems. Indus. Eng. Chem. Fund. 1,187–191.

[28]. Xu, J., Yu, B., Zou, M., &Xu, P. (2006). A new model for heat conduction of nanofluids based on fractal distributions of nanoparticles. J. Phys. D 39, 4486–4490.

[29]. Lin, K.C.,& Violi, A.(2010). Natural convection heat transfer of nanofluids in a vertical cavity: Effects of non-uniform particle diameter and temperature on thermal conductivity. Int. j. Heat Fluid Flow. 31, 236–245.

[30]. G.V. Hadjisophocleous, A.C.M. Sousa, J.E.S. Venart, Predicting the transient natural convection in enclosures of arbitrary geometry using a nonorthogonal numerical model, Numer. Heat Transfer: Part A 13 (1998) 373–392.

[31]. Tiwari, R.K.,& Das, M.K.(2007). Heat transfer augmentation in a two-sided lid-driven differentially heated square cavity utilizing nanofluids. Int. j. Heat Mass Trans. 50, 2002–2018.

[32]. T. Fusegi, K. Kuwahara, B. Farouk, A numerical study of threedimensional natural convection in a differentially heated cubic enclosure, Int. J. Heat Mass Transfer 34 (6) (1991) 1543–1557.

[33]. M.Y. Ha, M.J. Jung, A numerical study of three-dimensional conjugate heat transfer of natural convection and conduction in a differentially heated cubic enclosure with a heat-generating cubic conducting body, Int. J. Heat Mass Transfer 43 (2000) 4229–4248.